Dynamical properties of the hydration shell of fully deuterated myoglobin

Klaus Achterhold,[1] Andreas Ostermann,[2] Martine Moulin,[3] Michael Haertlein,[3] Tobias Unruh,[2,4] and Fritz G. Parak[1,*]

[1]*Physik-Department E17, Technische Universität München, James-Franck-Strasse 1, D-85747 Garching, Germany*

[2]*Forschungs-Neutronenquelle Heinz Maier-Leibnitz (FRM II), ZWE, Lichtenbergstrasse 1, D-85747 Garching, Germany*

[3]*ILL-EMBL Deuteration Laboratory, Partnership for Structural Biology, 6, rue Jules Horowitz, F-38042 Grenoble Cedex 9, France*

[4]*Institut für Physik der Kondensierten Materie, Lehrstuhl für Kristallographie und Strukturphysik, Staudtstrasse 3, D-91058 Erlangen, Germany*

(Received 24 May 2011; revised manuscript received 29 August 2011; published 25 October 2011)

Freeze-dried perdeuterated sperm whale myoglobin was kept in a water-saturated atmosphere in order to obtain a hydration degree of 335 ^1H_2O molecules per one myoglobin molecule. Incoherent neutron scattering was performed at the neutron spectrometer TOFTOF at the FRM II in an angular range of q from 0.6 to 1.8 Å^{-1} and a temperature range from 4 to 297 K. We used neutrons with a wavelength of $\lambda = 6$ Å and an energy resolution of about 65 μeV corresponding to motions faster than 10 ps. At temperatures above 225 K, broad lines appear in the spectra caused by quasielastic scattering. For an explanation of these lines, we assumed that there are only two types of protons, those that are part of the hydration water (72%) and those that belong to the protein (28%). The protons of the hydration water were analyzed with the diffusion model of Singwi and Sjölander [Phys. Rev. **119**, 863 (1960)]. In this model, a water molecule stays for a time τ_0 in a bound state performing oscillatory motions. Thereafter, the molecule performs free diffusion for the time τ_1 in a nonbound state followed again by the oscillatory motions for τ_0 and so forth. We used the general formulation with no simplifications as $\tau_0 \gg \tau_1$ or $\tau_1 \gg \tau_0$. At room temperature, we obtained $\tau_0 = 104$ ps and $\tau_1 = 37$ ps. For the protein bound hydrogen, the dynamics is described by a Brownian oscillator where the protons perform overdamped motions in limited space.

DOI: 10.1103/PhysRevE.84.041930 PACS number(s): 87.15.H−, 87.64.Bx, 68.35.Fx

I. INTRODUCTION

Proteins, the building blocks of life, are essential components of biological systems such as animals, plants, and micro-organisms. They are parts of complex systems. Isolated proteins very often become functionally inactive. This may be caused by a structural denaturation. But even with intact structure, a loss of their dynamic properties can destroy the function. Fortunately, a functionally active protein does not necessarily need the precise environment that it has in the biological system. In many cases, a water surrounding is sufficient for keeping a soluble protein active. Of special importance are the water molecules that are close to the surface of the protein. It has been shown that at least a belt of hydrogen-bridged water molecules is necessary to activate the protein dynamics [1,2]. Much work has been concentrated on myoglobin. This oxygen-binding protein contains a heme iron that can be used as a probe for protein dynamics. It allows the use of several spectroscopic methods. The correlation between hydration shell and dynamics has been shown by Mössbauer spectroscopy on the heme iron [3,4]. Frauenfelder and co-workers have investigated this correlation for three decades in several publications [5–7].

Incoherent neutron scattering has proven to be an excellent tool for studying the dynamics of bulk water [8], supercritical water [9], water in confined space [10], and hydration water [11]. However, measurements of hydration water of proteins yield an average over the mobility of all hydrogens in the sample, including the protons of the protein. Information about the dynamical behavior of the hydration shell of proteins becomes more directly accessible and therefore more accurate when fully deuterated protein samples are used. In perdeuterated proteins, all nonexchangeable ^1H atoms are replaced by deuterium (^2H). In a system of perdeuterated (^2H) protein, the ^1H_2O contribution of the hydration shell is predominant. Experimental investigations on the hydration shell of perdeuterated proteins have been performed with C-phycocyanin [12–14], maltose binding protein [15], and purple membrane [16]. For the following experiments, perdeuterated myoglobin was used. For the analysis of the experiments, two types of protons were distinguished: The water protons and the exchangeable hydrogens of the protein. There is no trial to identify different types of protons in the hydration water.

II. MATERIAL AND METHODS

Optimization of the expression and large-scale production of fully deuterated recombinant sperm whale myoglobin was carried out at the ILL-EMBL deuteration platform. Polymerase chain reaction (PCR) was performed on pMb413 using suitable primers and the PCR product cloned into pGEM-TeasyTM (Promega). After DNA sequencing, a NdeI-NotI fragment containing the myoglobin cDNA was cloned into the vector pET28a (Novagen), and the resulting expression construct pET28myo was transformed into *E. coli* BL21(DE3) cells. BL21(DE3) pET28myo cells were adapted to deuterated minimal medium and fed-batch fermentations of the adapted cells carried out [17]. A total of 77.5 g of perdeuterated cell paste have been obtained. Under these conditions, nearly all of the myoglobin was expressed in the apo form (without the heme group). Therefore, immediately after breaking up the *E. coli* cells by sonification and repeated thaw/freezing cycles, hemin (ferriprotoporphyrin IX cloride) was added to the solution to constitute the holo form of the myoglobin. As a first

*fritz.parak@ph.tum.de

purification step, fractionated ammonium sulfate participation (at levels of 55% and 95% ammonium sulfate) was performed. Already in this step, the remaining apomyoglobin could be eliminated. This was followed by an anion and subsequent cation exchange chromatography (Q- and SP-sepharose columns from Pharmacia) on a Pharmacia fast performance liquid chromatograph (FPLC). As a final purification step, the myoglobin was crystallized. The crystals were grown with the batch method from a solution of 2.9 M ammonium sulfate and 50 mM sodium phosphate at pH 5.8 containing 50 mg/mL myoglobin. To speed up the crystallization process, the crystallization batches were seeded with microfragments of a crashed myoglobin crystal with the space group $P2_1$. The crystals were collected and dissolved in distilled water. The myoglobin solution was desalinated and concentrated to a concentration of about 100 mg/mL by centrifugal filter devices (Centricon, Millipore Corp.). In the next step, the myoglobin solution was freeze-dried and subsequently dried further over silica gel in an exsiccator until no weight reduction through dehydration could be observed. The final amount of myoglobin was 60 mg. The hydration of the myoglobin sample was performed by replacing the silica gel by distilled water (^1H_2O). The hydration was controlled by an accuracy weighing machine and was stopped at a hydration degree of 335 water molecules per myoglobin molecule.

Sperm whale myoglobin contains 1265 hydrogen atoms. Of these, 282 are located in polarized bonds such as O-H and N-H in amino-acid side chains (136) or in the amid groups of the protein backbone (146). Since the purification and subsequent sample hydration process were carried out with ^1H_2O, nearly all of the exchangeable side-chain hydrogen atoms will have exchanged to ^1H. For the amid hydrogen atoms of the protein backbone, it is known from high-resolution neutron structure determination [18] that the degree of exchange depends on the flexibility or accessibility of the amid hydrogen position. From these data, the overall degree of exchange of amid hydrogen atoms can be calculated to be about 66% ^1H and 34% ^2H. Considering the 32 ^1H atoms of the heme group, we therefore can sum the ^1H atoms in the protein to 264 (side chains: 136, amid hydrogen: 96, and heme group: 32).

The measurements were carried out on the cold neutron multidisk-chopper time-of-flight spectrometer TOFTOF at the Forschungs-Neutronenquelle Heinz Maier-Leibnitz (FRM II) in Garching [19]. The incident wavelength was set to 6 Å and a chopper frequency of 12000 rpm was chosen that corresponds to an energy resolution of ~65 μeV (full width at half-maximum). The measurements were performed at temperatures between 4 and 297 K in a q range from 0.6 to 1.8 Å^{-1}. To correct for the scattering of the sample holder, we measured the empty sample holder at each temperature. The detector efficiency was corrected by a vanadium measurement. For the raw data processing, we used the program FRIDA (provided by Wuttke and Kargl: http://www.messen-und-deuten.de).

III. THEORY

The theory developed by Singwi and Sjölander is a general description of the diffusive motions in water [20]. In their model, a water molecule is trapped in a water cluster for a time τ_0 in the average. During this "residence time," it performs harmonic vibrations. After τ_0, it may jump from the trap into a "nonbound state" where it performs free diffusion for the time τ_1. After that time, it is trapped again in a cluster. In a scattering experiment with cold neutrons, the harmonic vibrations in the trap are taken into account by a Debye-Waller factor e^{-2W}. For their model, they gave a rigorous derivation of the dynamic scattering function. This analytic formulation of the theory was used for our analysis of the dynamics of the hydration shell of myoglobin performing a least-squares-fitting procedure.

In the Singwi-Sjölander model, the dynamic scattering function for neutron scattering is given by

$$S(q,\omega) = \frac{1}{\pi}\frac{e^{-2W}\tau_0}{1+\tau_1/\tau_0}\frac{\left(c+d\omega^2\tau_0^2\right)b}{b^2+\omega^2\tau_0^2\left(f+\omega^2\tau_0^2 g\right)}. \qquad (1)$$

In Eq. (1), the following abbreviations are used:

$$\begin{aligned} b &= 1+q^2D_1\tau_1-e^{-2W},\\ c &= 1+q^2D_1\tau_1+2\tau_1/\tau_0+\left(\tau_1^2/\tau_0^2\right)e^{2W},\\ d &= \left(\tau_1^2/\tau_0^2\right)e^{2W},\\ f &= (1+q^2D_1\tau_1)^2+\tau_1^2/\tau_0^2+2(\tau_1/\tau_0)e^{-2W},\\ g &= \tau_1^2/\tau_0^2,\\ 2W &= q^2\langle x_v^2\rangle. \end{aligned}$$

The energy and the momentum transfers are then given by $\hbar\omega = (\hbar^2/2m)(k_0^2-k_1^2)$ and $\hbar\vec{q} = \hbar(\vec{k}_0-\vec{k}_1)$, where m is the mass of the neutron. $\vec{k}_0$ and $\vec{k}_1$denote the initially and final wave vectors of the neutron, respectively. $\langle x_v^2\rangle$ gives the mean-square displacements, which exist even at very low temperatures. The free diffusion during τ_1 in the nonbound state is taken into account by D_1. If $\langle l^2\rangle$ is the mean-square displacement during τ_1, one obtains

$$D_1 = \langle l^2\rangle/6/\tau_1. \qquad (2)$$

The diffusion constant is given by

$$D = \frac{3\langle x_v^2\rangle+\langle l^2\rangle}{6(\tau_0+\tau_1)}, \qquad (3)$$

which contains the activation energy by τ_0 and τ_1.

While the Singwi and Sjölander theory describes the dynamics of water protons, we must also consider that not all hydrogen atoms of the protein are deuterons. Building up the hydration shell by normal water, the exchangeable deuteron atoms of the protein are replaced by protons. These protons can certainly not perform a free diffusion independent from the protein molecule. To correct for the motion of these protons, we used the Brownian oscillator model (compare, e.g., [21,22]). It was developed to understand protein dynamics measured by Mössbauer spectroscopy at the heme iron of myoglobin. Similar to the model of Singwi and Sjölander, the protein molecule is either trapped in a rigid state or it is in a flexible state. In the flexible state, segments of the protein perform Brownian motions. However, in contrast to the model of free diffusion, a back driving force ensures that the average protein

structure is conserved. As a result, we have an overdamped Brownian oscillator yielding the dynamic structure factor

$$S(q,\omega) = e^{-q^2\langle x_v^2\rangle} e^{-q^2\langle x_{\text{flex}}^2\rangle} \sum_{N=0}^{\infty} \frac{(q^2\langle x_{\text{flex}}^2\rangle)^N}{N!} \times \frac{N\hbar\alpha_{\text{flex}}/(2\pi)}{(\hbar\omega)^2 + (N\hbar\alpha_{\text{flex}}/2)^2}. \quad (4)$$

$\langle x_{\text{flex}}^2\rangle$ is the average mean-square displacement of segments of the molecule in the flexible state. The diffusive line broadening is measured by α_{flex}, which is connected with $\langle x_{\text{flex}}^2\rangle$by

$$\alpha_{\text{flex}} = c_{\text{flex}}\langle x_{\text{flex}}^2\rangle / T. \quad (5)$$

T is the temperature. c_{flex} is independent of T. The probability to explore the flexible state is given by

$$p(T) = \frac{1}{1 + e^{-\Delta G/R/T}} \quad (6)$$

with $\Delta G = \Delta H - T\Delta S$.

ΔH and ΔS are the enthalpy and the entropy differences between the rigid and the flexible state, respectively. R is the general gas constant.

IV. EXPERIMENTS AND RESULTS

We analyzed the experiments at 13 q values between 0.6 and 1.8 Å^{-1} and at nine temperatures. It has to be emphasized that Eqs. (1) and (4) have to be convoluted with the resolution of the neutron spectrometer before comparing with the experimental data. This experimental resolution function was taken from the myoglobin spectrum at $T = 4.2$ K and not from the measured vanadium spectrum to take into account sample volume and sample position effects. For the fitting procedure, we employed Eqs. (1)–(3) and (4)–(6) weighted by the fraction of water and protein bound hydrogen atoms, respectively. All 13 q-dependent spectra at a given temperature were included in one sole least-squares fit. To determine the solid-state vibrations, $\langle x_v^2\rangle$, we used spectra at $T = 4.2$, 50, 100, and 170 K, where no broad lines are present. The harmonic low-temperature values were linearly extrapolated to room temperature as proven by [23,24]. With these extrapolated $\langle x_v^2\rangle$ values, a Debye-Waller factor $e^{-q^2\langle x_v^2\rangle} = e^{-2W}$ was calculated for each temperature. The elastic scattering is reduced by this factor. The inelastic scattering by the solid-state vibrations below 1 meV is very small [25] compared to the remaining elastic and quasielastic scattering and was subtracted from the raw data. The free parameters for the dynamics of the hydration water molecules were τ_0, τ_1, and D_1. For the protein bound hydrogen atoms, we fitted α_{flex} in order to obtain c_{flex} according to Eq. (5). For their mean-square displacement,$\langle x_{\text{flex}}^2\rangle$, we used the values given by [26] for lysine protons in myoglobin. Figure 1 shows a spectrum taken at $T = 297$ K, $q = 1.7$ Å^{-1}. All contributions taken into account in the fitting procedure are shown. Figure 2 shows a selection of obtained experimental spectra together with the result of the least-squares fit. The fixed and the varied parameters for the spectra are listed in Table I.

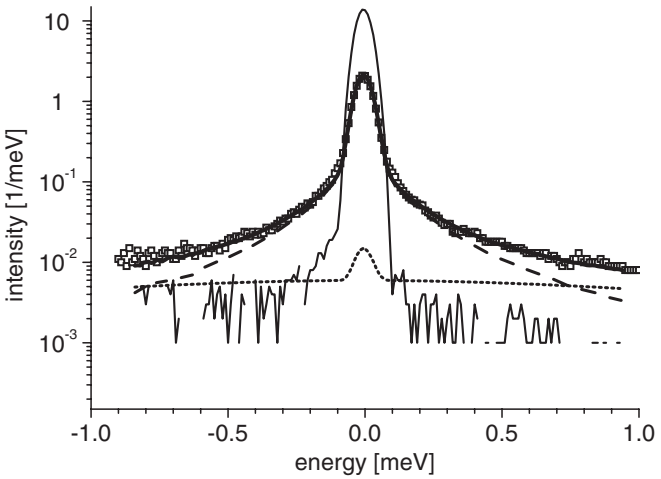

FIG. 1. Incoherent neutron scattering on perdeuterated myoglobin with a hydration shell of light water. $T = 297$ K, $q = 1.7$ Å^{-1}. Squares, experimental data; solid line, least-squares fit; dashed line, contribution of the water protons; dotted line, contributions of the protein protons; thin solid line, resolution function of the instrument.

V. DISCUSSION

Several theoretical approaches have been used for an analysis of incoherent neutron scattering. In the simplest case, free diffusion is described by a broadened Lorentzian where the width is determined by the diffusion constant [27]. Most authors apply so-called jump models. Essentially they describe diffusion as a jump from one trap to the next, surmounting the barrier between the traps in zero time. Examples in the literature can be found in [8,28–30]. Often the traps are limited within a sphere [31]. The jump model is a limiting case of the Singwi and Sjölander model with $\tau_1 \ll \tau_0$. Then, τ_0 is called residence time τ_{res}. To the best of our knowledge, no analysis using the unrestricted Singwi-Sjölander model is available in the literature.

From Table I, it is obvious that the dynamics of the hydration shell is determined by both τ_0 and τ_1. At room temperature, we obtained $\tau_0 = 104.1$ ps and $\tau_1 = 37.3$ ps. At this point, one has to discuss the energy resolution of the spectrometer and the physical meaning of τ_1 and τ_0. τ_1 is the time for being in the nonbound state. It is not connected with the characteristic time of motions in this state. The motions in the nonbound state determine the width of the quasielastic line. Figure 1 shows that the experimentally determined characteristic times are between 10 ps (resolution limit) and 0.66 ps (for the largest energy in Fig. 1). τ_0 is the average residence time of a water molecule in a trap. Jumps into the nonbound state occur only all 104.1 ps at room temperature. This is clearly not within the formal time resolution of the spectrometer. However, even if the resolution function of the spectrometer and of the experimental data cannot be separated, comparing their full width at half-heights, there is still information on τ_0 in the wings of the experimental spectra. Figure 3 may help us to understand this effect. The solid line gives the spectrum according Singwi and Sjölander, calculated with our fit parameters, but without convolution with the resolution of the spectrometer. The dashed and dotted lines show the same spectrum but with τ_0 changed by ±20%.

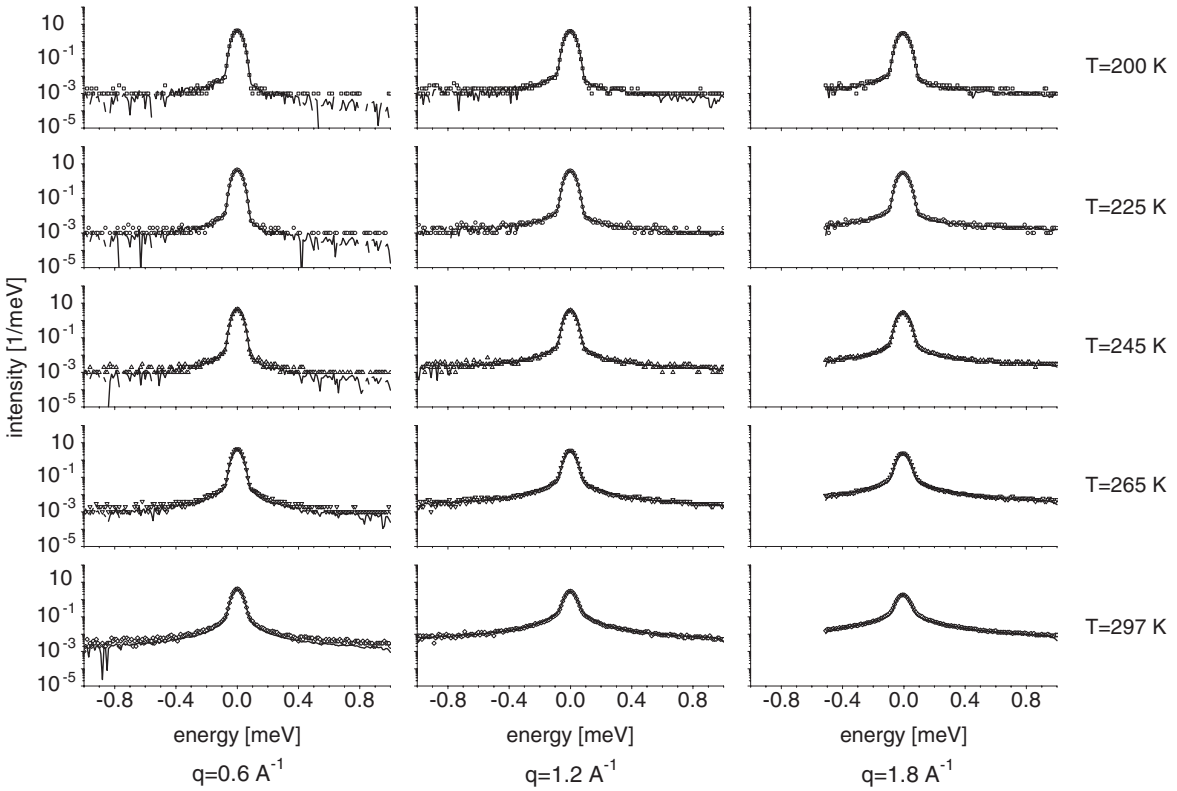

FIG. 2. Some typical spectra covering the temperature and the q range. Only the experimental data and the results of the fitting procedure (solid line) are given.

At full widths at half-height, the three plots look identical while the wings clearly differ. Considering the complete experimental spectrum allows us to determine τ_0, although it is not within the formal resolution. Our fit procedure using 13 complete spectra and only three free parameters allows us to obtain trustable τ_0 values.

It is interesting to compare our τ_0 with residence times in the literature. Bon [29] obtained 11 ps, while Jansson *et al.* [30] got 10.4 ps. More jumps yielding shorter residence times compensate in part for the missing free diffusion during τ_1. The square root of $\langle x_v^2 \rangle$ is a measure for the displacement by vibrations during the time τ_0 when the protons are trapped. At room temperature, it is only 0.036 Å^2 corresponding to a mean displacement of 0.19 Å. The mean-square displacement during τ_1 is measured by $\langle l^2 \rangle$ corresponding to a mean displacement of 4.3 Å. Similar values were found in [32]. The large value of $\langle l^2 \rangle$ may be astonishing at first glance. However, one has to have in mind that this value is not only a measure of the diffusion of the water molecule as a whole, but it is sensitive also to other mechanisms, such as a rotation of the water molecules.

D_1 considers the diffusion in the activated, nonbound state. It should depend on temperature. However, our fit shows that it has the same value at 297, 265, and 245 K. The values at 225 and 200 K suffer from large error bars. At these temperatures, the quasi-diffusive line nearly disappears, which explains the large error. Equation (2) shows that $\langle l^2 \rangle$ and τ_1 have to have the same temperature dependence to get a temperature-independent D_1. For a comparison with the literature, one has to use the diffusion constant D according to

TABLE I. Parameters obtained from the analyses of the experimental data by least-squares fit using Eqs. (1)–(6) and from the literature. τ_0, residence time in a trap; τ_1, time of free diffusion; $\langle x_v{}^2 \rangle$ values, mean-square displacements during τ_0 obtained from a linear extrapolation of low-temperature data; $\langle l^2 \rangle$ values, mean-square displacements during τ_1; D_1, diffusion constant during τ_1; D, effective diffusion constant. $\langle x_{\text{flex}}{}^2 \rangle$ according to Eq. (4) taken from [26]. The error-weighted value of c_{flex} of Eq. (5) became $(1.87 \times 10^{-4}) \pm (2.7 \times 10^{-6})$.

T (K)	τ_0 (ps)	τ_1 (ps)	$\tau_1/(\tau_0+\tau_1)$	$\langle x_v{}^2 \rangle$ (Å^2)	$D_1 \times 10^9$ (m^2/s)	$\sqrt{\langle l^2 \rangle}$ (Å)	$\langle x_{\text{flex}}{}^2 \rangle$ (Å^2)	$D \times 10^9$ (m^2/s)
297	104.1 ± 1.4	37.3 ± 0.9	0.2638	0.03636	0.83 ± 0.01	4.3	0.335	0.219
265	154.4 ± 1.6	21.3 ± 0.5	0.1212	0.03244	0.86 ± 0.02	3.3	0.238	0.104
245	254.5 ± 4.3	18.6 ± 0.8	0.0681	0.02999	0.86 ± 0.03	3.1	0.178	0.059
225	468 ± 18	19.6 ± 2.0	0.0402	0.02755	0.92 ± 0.07	3.3	0.117	0.006
200	561 ± 25	8.3 ± 3.2	0.0147	0.02448	1.85 ± 0.72	3.0	0.042	0.004

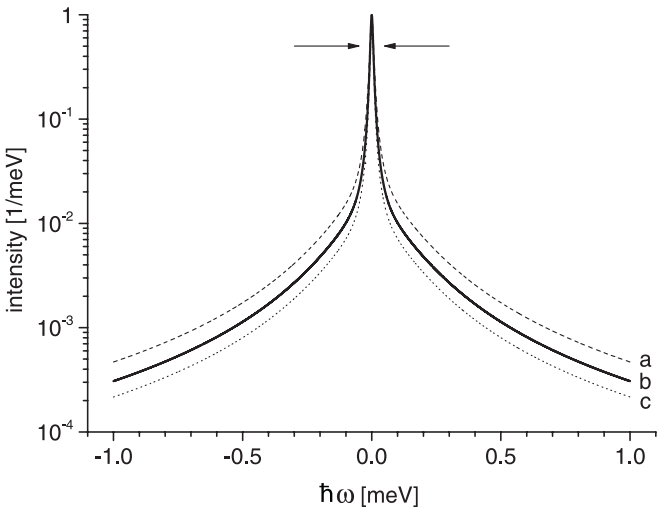

FIG. 3. Influence of a variation of τ_0 on the spectrum. Solid line *b*: Spectrum according to Singwi-Sjölander with the obtained fit parameters at room temperature, no convolution with the resolution of the spectrometer, $\tau_0 = 104$ ps. For curves *a* and *c*: τ_0 is changed by ±20%. Note the logarithmic scale. The full width at half-height is indicated by arrows. Although the three spectra cannot be distinguished at full width at half-height, their wings are separated.

Eq. (3). At room temperature, D of bulk water equals 2.299×10^{-9} m^2/s [33]. We obtained 0.219×10^{-9} m^2/s for the hydration water and the common decrease with temperature, which looks reasonable. Jansson *et al.* [30] obtained 0.74×10^{-9} m^2/s for a water-glycerol mixture on myoglobin. Bon [29] got 0.25×10^{-9} m^2/s for hydration water on lysozyme, in good agreement with our value. NMR investigations yielded D equal to 1×10^{-9} m^2/s for the hydration water on myoglobin [34]. The larger value may be a consequence of the different time sensitivity compared to QENS. MD calculations also yield larger values [35,36].

From the temperature dependence of the ratio τ_0/τ_1, one can determine the activation energy, which is necessary to reach the free diffusion state. The probability to reach this state is given by Eq. (7) with

$$\exp[(\Delta H - \Delta ST)/R/T] = \tau_0/\tau_1. \tag{7}$$

ΔH and ΔS are the enthalpy and the entropy differences between the two states, respectively.

The obtained value is given in Table II column 2 (hydration H_2O). The data of Table II allow us to estimate a reaction constant for the jump from state 0 to state 1 within the hydration shell:

$$K_{01} = \frac{k_B T}{h} e^{-(\Delta H/RT)} e^{\Delta S/R} = K e^{-\Delta H/RT}, \tag{8}$$

where k_B is the Boltzmann number and h is the Planck constant. For room temperature, we get $K = 1.38\ 10^{15}$ s^{-1}. This can be compared to the activation of β relaxation of the hydration shell obtained from dielectric relaxation spectroscopy on a sample with $h = 0.4$ (g water/g myoglobin [7]). The values $\Delta H = 79.2$ kJ/mol and $K = 10^{20.5}$ s^{-1} are much larger than those obtained from incoherent neutron scattering. The discrepancy may be due to the different time sensitivity of the two methods. While dielectric relaxation spectroscopy covered a frequency region up to about 10^{10} Hz, which corresponds to a time sensitivity up to 100 ps, the neutron experiments described here were sensitive for processes faster than several picoseconds. Entropy enthalpy compensation is more likely. While K_{01} becomes 2×10^{12} s^{-1} for the neutron experiment, it is 7×10^{11} s^{-1} in the case of the permittivity measurements. As already mentioned, the dynamics of the protein bound protons was analyzed within the model of a Brownian oscillator. The activation energy to come from the rigid state to the flexible state was obtained from the temperature dependence of the $\langle x^2_{\text{flex}}\rangle$ values taken from [26],

$$\langle x^2_{\text{flex}}\rangle = \frac{c_{\text{flex}} T}{1 + e^{\Delta H/RT} e^{-\Delta S/R}}. \tag{9}$$

The activation enthalpy is slightly higher than that for free water protons. However, the entropy difference is clearly larger. This means that the protein protons stay for a longer time in the flexible state compared to the water protons in their excited state.

Protein-specific motions as measured by the heme iron have a higher activation enthalpy. This may be due to the fact that these motions involve segments of the molecule that have larger masses. Their entropy difference is practically the same as that for protein bound protons. It results in a relatively high probability for the system to stay in the flexible state.

It is interesting to note that the activation energy for the protein dynamics as measured at the iron by Mössbauer spectroscopy is of the same order as that for the protein protons or even the hydration protons. Water protons, protein protons, and other components including the heme group build a strongly coupled system in which hydrogen bridges are essential components for their stability.

TABLE II. Activation energies of hydration protons (column 2) and protons as part of the myoglobin molecule (column 3). For comparison, we added data obtained by Mössbauer spectroscopy on the heme iron (from [22]). They represent the difference in free Gibbs energy between the so-called flexible state and the rigid state (column 4).

	Hydration H_2O	Protein H	Heme Fe
ΔH (kJ/mol)	16.17	17.8	21 ± 0.96
ΔS (kJ/mol/K)	0.045	0.075	0.080 ± 0.004

VI. CONCLUSIONS

Fifty years ago, Singwi and Sjölander formulated an analytic theory for self-diffusion in water. The limiting case of this theory assuming jumps between traps in zero time was successfully applied for an analysis of the diffusion in the hydration shell of proteins. We have shown that the unrestricted theory is well suited to describe the diffusion within the hydration shell of a protein. It is interesting to compare the model of Singwi and Sjölander with the model of the Brownian oscillator. In both models, one has two states: a trap or a rigid state and the state of free diffusion or the flexible state, respectively. The only difference is the addition of a back driving force in the case of the Brownian oscillator. While in

the free diffusion there is no limit for the displacements, the diffusion in the Brownian oscillator is limited in space.

ACKNOWLEDGMENTS

The authors wish to thank Sebastian Busch for valuable discussions and support for the data-reduction program FRIDA. This work has benefited from the activities of the DLAB consortium funded by the EU under Contracts No. HPRI-2001-50065 and No. RII3-CT-2003-505925, and from UK EPSRC-funded activity within the ILL-EMBL Deuteration Laboratory under Grants No. GR/R99393/01 and No. EP/C015452/1. F.G.P. thanks the Fond der Chemie for support.

[1] G. Careri, A. Giansanti, and J. A. Rupley, Proc. Natl. Acad. Sci. USA **83**, 6810 (1986).
[2] M. Peyrard, J. Biolog. Phys. **27**, 217 (2001).
[3] G. P. Singh, F. Parak, S. Hunklinger, and K. Dransfeld, Phys. Rev. Lett. **47**, 685 (1981).
[4] F. Parak, in *Biomembranes*, edited by L. Packer, Vol. 127 (Academic, Orlando, 1986), p. 196.
[5] H. Frauenfelder and E. Gratton, in *Biomembranes*, edited by L. Packer, Vol. 127 (Academic, Orlando, 1986), p. 207.
[6] P. W. Fenimore *et al.*, Proc. Natl. Acad. Sci. USA **99**, 16047 (2002).
[7] H. Frauenfelder *et al.*, Proc. Natl. Acad. Sci. USA **106**, 5129 (2009).
[8] J. Teixeira, M.-C. Bellissent-Funel, S. H. Chen, and A. J. Dianoux, Phys. Rev. A **31**, 1913 (1985).
[9] T. Tassaing and M.-C. Bellissent-Funel, J. Chem. Phys. **113**, 3332 (2000).
[10] S. Mitra *et al.*, J. Phys. Condens. Matter **13**, 8455 (2001).
[11] M.-C. Bellissent-Funel, J. Mol. Liq. **84**, 39 (2000).
[12] S. Dellerue and M.-C. Bellissent-Funel, Chem. Phys. **258**, 315 (2000).
[13] W. Doster, S. Busch, A. M. Gaspar, M. S. Appavou, J. Wuttke, and H. Scheer, Phys. Rev. Lett. **104**, 098101 (2010).
[14] F. Gabel and M. Bellissent-Funel, Biophys. J. **92**, 4054 (2007).
[15] K. Wood *et al.*, J. Am. Chem. Soc. **130**, 4586 (2008).
[16] K. Wood *et al.*, Proc. Natl. Acad. Sci. USA **104**, 18049 (2007).
[17] J.-B. Artero *et al.*, Acta Crystallogr. Sect. D **61**, 1541 (2005).
[18] A. Ostermann *et al.*, Biophys. Chem. **95**, 183 (2002).
[19] T. Unruh, J. Neuhaus, and W. Petry, Nucl. Instrum. Methods Phys. Res., Sect. A **580**, 1414 (2007).
[20] K. S. Singwi and A. Sjölander, Phys. Rev. **119**, 863 (1960).
[21] F. Parak, E. W. Knapp, and D. Kucheida, J. Mol. Biol. **161**, 177 (1982).
[22] M. Schmidt *et al.*, Eur. Biophys. J. **38**, 687 (2009).
[23] G. U. Nienhaus *et al.*, Nature (London) **338**, 665 (1989).
[24] F. Parak *et al.*, Hyperfine Interact. **71**, 1319 (1992).
[25] A. Paciaroni, A. Orecchini, E. Cornicchi, M. Marconi, C. Petrillo, M. Haertlein, M. Moulin, H. Schober, M. Tarek, and F. F. Sacchetti, Phys. Rev. Lett. **101**, 148104 (2008).
[26] N. Engler *et al.*, Proc. Natl. Acad. Sci. USA **100**, 10243 (2003).
[27] M. Bee, *Quasi Elastic Neutron Scattering. Principles and Applications in Solid State, Chemistry, Biology and Material Sciences* (Adam Hilger, Bristol, 1988).
[28] A. Paciaroni, S. Cinelli, and G. Onori, Biophys J. **83**, 1157 (2002).
[29] C. Bon *et al.*, Biophys. J. **83**, 1578 (2002).
[30] H. Jansson *et al.*, J. Chem. Phys. **130**, 205101 (2009).
[31] M. Tehei and G. Zaccai, FEBS. J. **274**, 4034 (2007).
[32] J. Fitter *et al.*, Proc. Natl. Acad. Sci. USA **93**, 7600 (1996).
[33] R. Mills, J. Phys. Chem. **77**, 685 (1973).
[34] K. Kotitschke *et al.*, Prog. Colloid Polym. Sci. **83**, 211 (1990).
[35] I. Muegge and E. W. Knapp, J. Phys. Chem. **99**, 1371 (1995).
[36] M. Marchi, F. Sterpone, and M. Ceccarelli, J. Am. Chem. Soc. **124**, 6787 (2002).